Netsu Sokutei **27** (2) 100-104

解 説

High-temperature Calorimetry of Fusion Reactor Blanket Materials

Heiko Kleykamp

(Received February 14, 2000; Accept February 23, 2000)

The experimental techniques of high-temperature heat flow calorimetry are explained in view of selection and mass optimisation of standards for caloric calibration, condition of samples, heating rates and liner materials. Calorimetric work is illustrated on enthalpy measurements of Li_4SiO_4, Li_2SiO_3, Li_2ZrO_3, $LiAlO_2$ and Li_2TiO_3 by isothermal drop calorimetry and by heat capacity calculations therefrom. The physics of second-order transitions is discussed taking Li_4SiO_4 as an example. An additional enthalpy uptake occurs in the critical temperature range under anisothermal conditions. The behaviour is reversible. The anisothermal calorimetry is further outlined by measurements of the enthalpy of solidification of Li_4SiO_4 and the enthalpy of transformation and melting of beryllium.

1. Introduction and experimental aspects

Differential thermal analysis (DTA) and heat flow calorimetry are powerful and complementary methods in the field of high-temperature phase equilibria and thermodynamics. Commercial DTA apparatus are simple to handle, can be operated up to 2400℃ and are characterised by a short time constant of the signal less then 30 s. Hence, closely located peaks are easily separated by DTA during heating and cooling. An example is given in Ref.1 for a 50 mg beryllium sample at a heating rate 2 K min^{-1}. The hexagonal close-packed structure undergoes a transformation at 1269℃ to the body-centred cubic modification which melts at 1283℃. The difference are 14 degrees. The shoulder observed on the lower temperature peak can be related to a eutectic melting of beryllium with beryllium-impurity compounds at 1282℃.[1)]

The handling of high-temperature calorimeters for caloric measurements is more difficult due to the calibration procedures. Qualified commercial instruments are differential scanning calorimeters and heat flow calorimeters operating up to 1550℃ or even higher. We have well-founded experience with the latter, an HTC 1800 type of SETARAM S. A., Lyon. The instrument operates according to the heat flow principle either in the isothermal mode by dropping a sample at 25℃ into a preheated crucible or in the anisothermal mode by linear heating or cooling of a sample positioned in a preheated crucible. Enthalpy measurements are calibrated with the enthalpy of synthetic α-Al_2O_3 spheres using the JANAF Thermochemical Tables.[2)] Latent heat determinations (enthalpies of transformation, melting, reaction) are preferably calibrated with tabulated enthalpies of melting of selected elements, *e.g.*, Al, Au, Cu, Ni, Pd.[3)] We found out that the calibration by measurements of the enthalpy $H^\circ_T-H^\circ_{298}$ and the enthalpy of transition ΔH°_T result in different sensitivity factors S_T at given temperatures, see **Fig.1**. These factors are strongly temperature dependent and are defined by

$$S_T=\frac{Q_T}{H^\circ_T-H^\circ_{298}}\cdot\frac{M}{m} \qquad (1)$$

and

Paper presented at the 35th Japanese Conference on Calorimetry and Thermal Analysis, Tokyo, 10 - 12 November 1999.

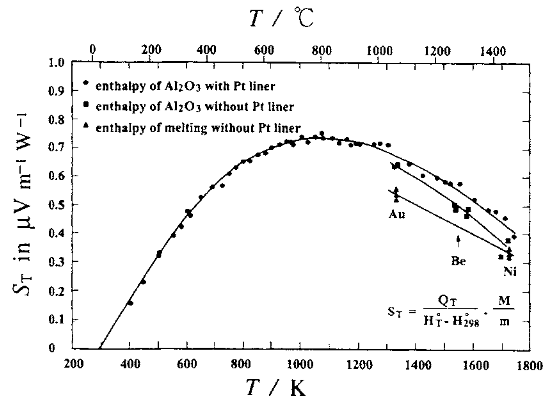

Fig.1 Calibration of the SETARAM HTC 1800 calorimeter with the enthalpy of α-Al_2O_3 and the enthalpy of melting of Au and Ni.

$$S_T = \frac{Q_T}{\Delta H^\circ_T} \cdot \frac{M}{m} \tag{2}$$

where Q_T is the area of the registered heat signal in μV·s. The relative atomic mass is marked by M and m is the mass of the sample. The detector is made up of two alumina crucibles, one above the other, which are surrounded by two crown-shaped piles of 18 plus 18 Pt-6 % Rh/Pt-30 % Rh thermocouples (EL 18), each pile in one plane.[4] A platinum liner inside the crucibles results in lower standard errors of the measurements on ceramic materials due to a more symmetric radial heat transport. However, the incompatibility of platinum with many metals and alloys rules out the use of this liner material. A remedy could be a platinum liner squeezed onto the outer surface of the alumina crucibles. The application of a liner necessitates a separate calibration, see **Fig.1**. The time constant of the calorimeter signal is about 5 min. A heating rate of 2 K min^{-1} is reasonable. Heating rates of 0.5 K min^{-1} and lower result in growing instabilities of the heat flow curve. The optimum mass range of standards and samples is 50 to 200 mg depending on their relative atomic masses. The enthalpies and the latent heats of standard and sample should be of the same order of magnitude. Therefore, low masses should be used for specimens and standards with low relative atomic masses compared to the masses of those with high relative atomic masses in order to get comparable Q values of standard and specimen.

Table 1 Heat capacities C_p of selected ceramic breeder materials and temperature range of the measured enthalpies.

compound	C_p in J K^{-1}mol^{-1} 298 K	1100 K	temperature range of measurements in K	ref.
Li_4SiO_4	182.1	304.2	298 ~ 1300	5)
Li_2SiO_3	95.4	160.6	298 ~ 1414	6)
Li_2ZrO_3	120.4	149.8	298 ~ 1410	6)
$LiAlO_2$	65.8	103.1	298 ~ 1673	7)
Li_2TiO_3	108.6	154.1	298 ~ 1650	8)

2. Enthalpy and heat capacity

Enthalpy measurements were made on Li_4SiO_4,[5] Li_2SiO_3,[6], Li_2ZrO_3,[6], $LiAlO_2$[7] and Li_2TiO_3[8] between about 380 and 1673 K in the isothermal mode by the drop method. Experiments at lower temperatures are not advisable because the heat flow becomes too low. The upper temperature limit is fixed by the evaporation of the sample and should not increase further when a mass loss of 0.5 % is attained after the respective experiment. The standard deviation of the enthalpy measurements is better than 3 %. Heat capacities are obtained by differentiating the fitted enthalpy curves $H^\circ_T - H^\circ_{298} = a + b \cdot T + c \cdot T^2 + d \cdot T^{-1}$. This method is successful in the temperature regions where no second-order transitions occur. Examples of the heat capacities measured in the field of fusion reactor ceramic breeder materials are compiled in **Table 1**. The Dulong-Petit rule is fulfilled for these materials at about 1100 K resulting in C_p = 25 JK^{-1} g-atom^{-1} with the exception of Li_4SiO_4 which is characterised by additional vibrations and rotations of molecule groups above the second-order transitions at 938 K and 996 K.[5]

3. First-order and second-order transitions

Examples for first-order transitions of solid compounds are transformations from one to another crystal structure or the congruent melting processes. These phenomena occur at distinct temperatures T_{tr} and T_m, resp., where both phases are in thermodynamic equilibrium. The heat capacity becomes infinite, enthalpy and entropy are discontinuous, the Gibbs energy is continuous, but not differentiable at these temperatures. A second-order transition proceeds steadily in a

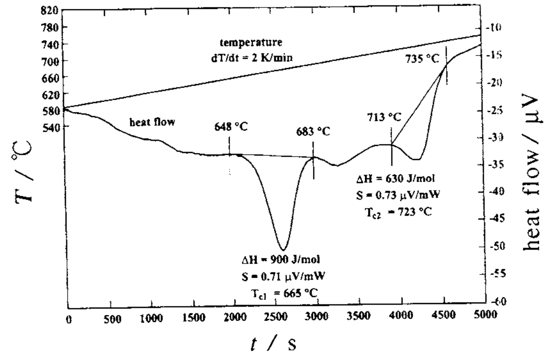

Fig.2 Heat flow curve in the region of the critical temperatures T_{c1} and T_{c2} of Li_4SiO_4. The curve proves an additional enthalpy uptake of 900 J mol^{-1} and 630 J mol^{-1}, resp.

temperature region by uptake of additional heat from the surroundings for the generation of structural, magnetic, electric, etc. disorder. This is connected with a finite increase of the heat capacity up to a maximum value at the critical temperature T_c. The temperature behaviour is reversible. Enthalpy, entropy and Gibbs energy remain continuous and differentiable functions in this temperature region whereas the heat capacity is continuous, but it is not differentiable. The disordered fraction of C_p above the basic $C_p(T)$ curve, δC_p, can be calculated according to Becker9) by introduction of an order parameter, attaining a maximum value of $\delta C_p = 3R/2$ at T_c. The heat capacity should drop steeply to the basic $C_p(T)$ curve above T_c. In this temperature region, however, some short-range order remains which is expressed in the $C_p(T)$ curve by a slow decrease due to further heat consumption for the residual short range order above T_c. There is no two-phase equilibrium at the critical temperature. Excellent examples for the heat capacity curves in the regions of first-order and second-order transitions are illustrated in Ref. 10.

The enthalpy and the entropy of transition are zero for a second-order transition. Nevertheless, a signal develops also by DTA which is based on the additional heat flow from the surroundings to the sample in the heating mode. The signal increases steadily up to T_c and differs distinctly from the signal of a first-order transition. The different peak shapes and the reversible behaviour are illustrated in Ref. 5 for cobalt with a first-order structural hcp → fcc transition at 422 ℃ and a second-order ferromagnetic- paramagnetic transition at 1121 ℃.

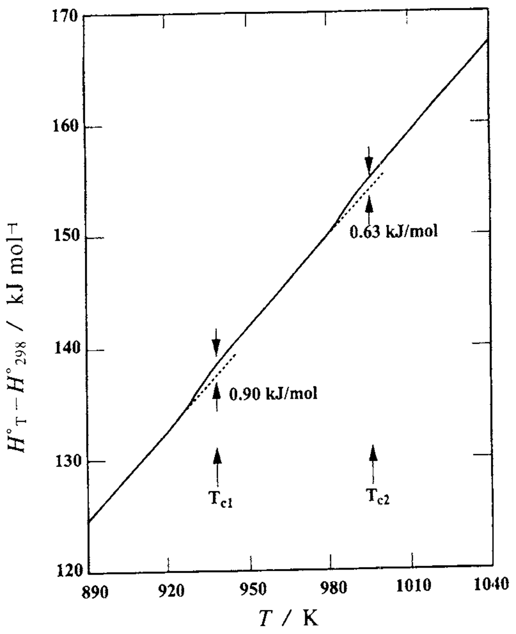

Fig.3 Enthalpy of Li_4SiO_4 in the region of the second-order transitions at T_{c1} and T_{c2}.

Li_4SiO_4 has two second-order transitions which were investigated by differential scanning calorimetry11,12) and by drop calorimetry using the quasi-local linear regression method.13) Second-order transitions are quantitatively evidenced by heat flow calorimetry in the anisothermal mode. **Fig.2** illustrates the additional enthalpy uptake in the second-order transition regions of Li_4SiO_4. The first transition becomes noticeable at 648 ℃ and is terminated at 683 ℃. The extremum of the heat flow is located at 665 ℃ which is the critical temperature of the first transition. The second transition starts at 713 ℃ and vanishes at 735 ℃. The heat flow curve passes the extremum at 723 ℃, the critical temperature of the second transition. The endothermal peaks develop gradually during heating. The heat flow integration and the calibration result in an additional enthalpy uptake of 900 J mol^{-1} and 630 J mol^{-1}, resp. The enthalpy of Li_4SiO_4 in the temperature interval 890 ~ 1040 K is illustrated in **Fig.3**. The enthalpy curve is a continuous and differentiable function in the region of the critical temperatures T_{c1} = 938 K and T_{c2} = 996 K. The points of inflection in the $H(T)$ curve mark the critical

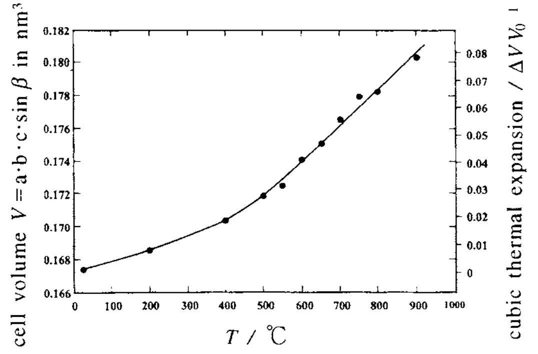

Fig.4 Cell volume and cubic thermal expansion of Li_4SiO_4 as a function of temperature.

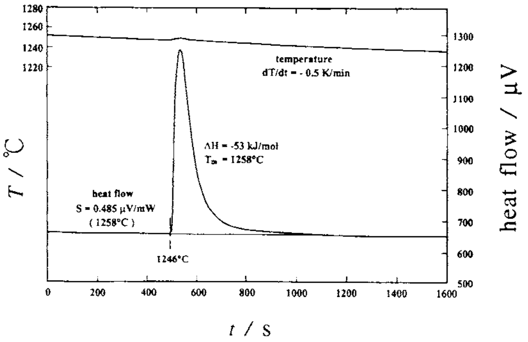

Fig.5 Enthalpy of solidification of undercooled Li_4SiO_4.

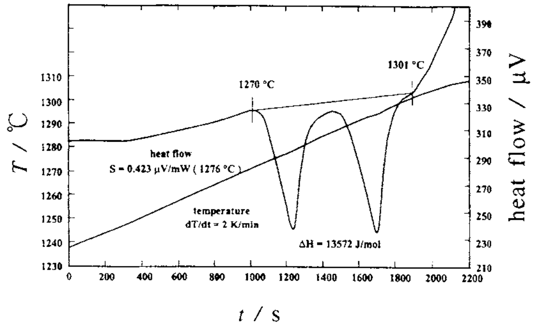

Fig.6 Enthalpies of transformation and melting of beryllium.

temperatures T_C. The reasons for the second-order transitions are unknown: excitations of vibrations or rotations of molecule groups or ferroelectric-paraelectric transitions are possible.

Furthermore, lattice parameter measurements have been made on Li_4SiO_4 powder by high-temperature X-ray diffractometry up to 900℃ in 50 degrees steps.[14] The lattice parameters a and b are monotonous functions of temperature whereas c shows a shallow dip in the temperature region 600～750℃. The angle $\beta = 90.3°$ of the monoclinic cell is independent of temperature. The cell volume $V = a \cdot b \cdot c \cdot \sin\beta$ turns out to be a monotonous function of temperature, it is presented in **Fig.4**. The cubic thermal expansion $\Delta V V_0^{-1}$ of Li_4SiO_4 is added to the figure. The reference temperature is 20℃. The development of the curve is non-linear, but it is continuous and does not point to a first-order transition.

4. Enthalpies of transformation and melting

The present measurements of the enthalpy of melting are focused on the breeder material Li_4SiO_4 and the neutron multiplier beryllium within the field of the fusion reactor blanket material development. The Li_4SiO_4 samples in the 100 mg range were encapsulated in thin platinum foils in order to reduce the increasing Li_2O evaporation during heating above 1000℃. The calibration was done with the enthalpy of solidification values of gold and nickel by interpolation to the melting point of Li_4SiO_4 at 1258℃.[15] The masses of the standards have to be adjusted to the mass of the specimen to make the heat consumption Q (in μV s) comparable for specimen and standards. In general, the enthalpy of melting curves are more reproducible. However, in the case of Li_4SiO_4 the enthalpy of solidification curves are more aesthetic though undercooling has to be considered, see **Fig.5**. The temperature of solidification of the undercooled liquid at a rate $dT/dt = -0.5$ K min^{-1} is 1246℃ in the experiment. Therefore, the difference of the enthalpy $H°_{1258} - H°_{1246}$ between this temperature and the thermodynamic melting temperature ($=4$ kJ mol^{-1}) has to be added to the absolute value of the enthalpy of solidification resulting in the enthalpy of melting $\Delta_{fus}H = (53 \pm 4)$ kJ mol^{-1} at 1258℃.

The determination of the enthalpies of transformation and melting of beryllium is more demanding because the corresponding temperatures are only 14 degrees separate and the time constant of the calorimeter signal is about 5 min. It was not advisable to use commercially available beryllium spheres with small diameters ≤ 2 mm because the surface-to-volume ratio is unfavourable due to the oxidation sensitivity and the passivation of the material; further, the heat sinks were spatially distributed on the crucible bottom during heating and the coalescence of many small spheres to one big sphere was hindered during the melting process. Therefore, thin beryllium disks were used and were positioned on the flat bottom of the Al_2O_3 crucible. The system is thermodynamically incompatible; however, reactions have not been observed. The heating rate of the experiment was $2\ K\ min^{-1}$. The result is illustrated in **Fig.6**. The calorimeter was switched off at 1300℃ in order to avoid a long-time period of molten beryllium. The two overlapping peaks were separated by a special calorimeter software. The enthalpy of the hcp → bcc transformation results in $\Delta_{tr}H = (6.1 \pm 0.5)\ kJ\,mol^{-1}$, the enthalpy of melting gives $\Delta_{fus}H = (7.2 \pm 0.5)\,kJ\,mol^{-1}$.[1] The values are comparable in their extent.

5. Conclusions

Enthalpies and latent heats of inorganic materials can be measured easily by commercial heat flow calorimeters up to 1500℃. The standard deviation of enthalpies is better than 3 %, the standard deviation of latent heats is larger due to interpolation and to limitation of standards with appropriate transition temperatures and precise enthalpies of transition. The shape of the DTA and calorimeter signals indicates the order of transition. The second-order transitions of Li_4SiO_4 are presented by an additional heat uptake, the behaviour is reversible during cooling. The minima in the heat flow curve and the points of inflection in the enthalpy vs. temperature curve characterise the critical temperatures T_c where the gradual disorder process is completed during heating.

References

1) H. Kleykamp, *Thermochim. Acta* **345,** 179 (2000).
2) M. W. Chase, NIST-JANAF Thermochemical Tables, 4th Ed., AIP, Woodbury, New York (1998).
3) A. T. Dinsdale, NPL report DMA (A) 1995 (1989).
4) J. Mercier, *J. Thermal Anal.* **14,** 161 (1978).
5) H. Kleykamp, *Thermochim. Acta* **287,** 191 (1996).
6) H. Kleykamp, *Thermochim. Acta* **237,** 1 (1994).
7) H. Kleykamp, *J. Nucl. Mater.* **270,** 372 (1999).
8) H. Kleykamp, unpublished.
9) R. Becker, Theorie der Wärme, 3rd edn. Springer, Berlin (1985).
10) I. Hatta, *Pure Appl. Chem.* **64,** 79 (1992).
11) G. W. Hollenberg, *J. Nucl. Mater.* **103-104,** 591 (1981).
12) R. Brandt and B. Schulz, *J. Nucl. Mater.* **152,** 178 (1988).
13) A. Asou, T. Terai, and Y. Takahashi, *J. Chem. Thermodyn.* **24,** 273 (1992).
14) A. Skokan, unpublished results (1985).
15) S. Claus, H. Kleykamp, and W. Smykatz-Kloss, *J. Nucl. Mater.* **230,** 8 (1996).

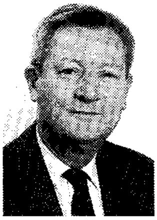

Heiko Kleykamp
Forschungszentrum Karlsruhe, Institut für Materialforschung I, Postfach 3640, 76021 Karlsruhe, Germany
Tel: +49-7247-82-2888
Fax: +49-7247-82-4567
e-mail: heiko.kleykamp@imf.fzk.de